

Conflict-Aware Multimodal Fusion for Ambivalence and Hesitancy Recognition

Salah Eddine Bekhouche

University of the Basque Country UPV/EHU, San Sebastian, Spain

bekhouchesalah@gmail.com

Hichem Telli

Laboratory of LESIA, University of Biskra, Algeria

tellihicham@univ-biskra.dz

Azeddine Benlamoudi

Lab. de Génie Electrique (LAGE), University Kasdi Merbah Ouargla, Ouargla, Algeria

benlamoudi.azeddine@univ-ouargla.dz

Salah Eddine Herrouz

Lab. de Génie Electrique (LAGE), University Kasdi Merbah Ouargla, Ouargla, Algeria

herrouz.salaheddine@univ-ouargla.dz

Abdelmalik Taleb-Ahmed

Institute of Electronics, Microelectronics and Nanotechnology (IEMN),
Polytechnic University of Hauts-de-France, University of Lille, Valenciennes, France

abdelmalik.taleb-ahmed@uphf.fr

Abdenour Hadid

Sorbonne Center for Artificial Intelligence, Sorbonne University Abu Dhabi, UAE

abdenour.hadid@sorbonne.ae

Abstract

Ambivalence and hesitancy (A/H) are subtle affective states where a person shows conflicting signals through different channels—saying one thing while their face or voice tells another story. Recognising these states automatically is valuable in clinical settings, but it is hard for machines because the key evidence lives in the disagreements between what is said, how it sounds, and what the face shows.

*We present **ConflictAwareAH**, a multimodal framework built for this problem. Three pre-trained encoders extract video, audio, and text representations. Pairwise conflict features—element-wise absolute differences between modality embeddings—serve as bidirectional cues: large cross-modal differences flag A/H, while small differences confirm behavioural consistency and anchor the negative class. This conflict-aware design addresses a key limitation of text-dominant approaches, which tend to over-detect A/H (high F1-AH) while struggling to confirm its absence: our multimodal model improves F1-NoAH by +4.6 points over*

text alone and halves the class-performance gap. A complementary text-guided late fusion strategy blends a text-only auxiliary head with the full model at inference, adding +4.1 Macro F1.

*On the BAH dataset from the ABAW10 Ambivalence/Hesitancy Challenge, our method reaches **0.694 Macro F1** on the labelled test split and **0.715** on the private leaderboard, outperforming published multimodal baselines by over 10 points—all on a single GPU in under 25 minutes of training.*

1. Introduction

Ambivalence is when someone holds conflicting feelings about the same thing at the same time. Hesitancy is closely related: it is the reluctance or the delay before committing to a decision. Both states come up frequently in clinical psychology, behavioural economics, and human-computer interaction, yet they remain difficult to detect automatically.

Why is this clinically important? In medical interviews,

a patient may agree to a treatment plan verbally but show signs of doubt or stress on their face. Catching this mismatch early can help clinicians adjust their approach—for instance during motivational interviewing [17]—or flag attitudes linked to vaccine hesitancy [6] and treatment refusal.

From a computational point of view, A/H is different from the “Big 6” basic emotions. Happiness or anger tend to show up clearly through a single channel: facial action units, prosody, or word choice. A/H, on the other hand, often produces *contradictory* cross-modal signals. A person says “I feel fine” while their voice wavers. Their words express agreement, but micro-expressions betray uncertainty. Standard multimodal fusion methods are designed to find what the modalities *agree* on; they can actually suppress the disagreement signals that define A/H.

The ABAW10 Ambivalence/Hesitancy Video Recognition Challenge [13] provides a benchmark to study this problem. It uses the BAH dataset [7]: 1,427 clinical interview videos from 300 participants, annotated at the video level with binary A/H labels. With only 778 training videos and expert-level annotations that are expensive to obtain, the dataset is intentionally small—making regularisation and pre-trained representations essential.

Our contributions are as follows:

1. **Conflict-aware multimodal fusion.** We introduce explicit pairwise conflict features that act as *bidirectional* cues: large cross-modal differences flag A/H, while small differences anchor the negative class. This corrects the systematic class bias of text-dominant approaches: our conflict-aware model improves F1-NoAH by +4.6 points over text alone and halves the class-performance gap—a crucial property for clinical deployment where false-positive A/H flags waste clinician time.
2. **Text-guided late fusion.** A text-only auxiliary head is blended with the full multimodal output at inference, adding +4.1 Macro F1 by leveraging the strong linguistic signal while keeping multimodal evidence for ambiguous cases.
3. **Efficient, reproducible baseline.** Our full pipeline trains in under 25 minutes on a single NVIDIA RTX 4090, yet outperforms published multimodal baselines by more than 10 points and achieves 0.715 Macro F1 on the official ABAW10 leaderboard.

2. Related Work

Affective Behaviour Analysis and the ABAW Challenges. The Affective Behaviour Analysis in-the-Wild (ABAW) workshop series has been a principal driver of progress in multimodal affective computing, defining benchmarks for facial action unit (AU) detection, valence-arousal estimation, and discrete expression recognition [12]. The eighth edition introduced the Ambivalence/Hesitancy (A/H) Recognition Challenge, marking the

first large-scale benchmark for this clinically motivated task [12, 13]. The tenth edition (ABAW10) [13] continues this track with the full BAH dataset [7], providing participant-wise train/val/test splits and an additional unlabelled hold-out for challenge evaluation.

Several teams competed in ABAW-8. Savchenko [24] achieved the highest reported Macro F1 of 0.772 using a text-dominant approach: frame-level visual emotion features were aggregated statistically and combined with transcript embeddings, with the linguistic modality contributing the decisive gain. This result established text as the primary carrier of A/H information. Hallmen et al. [8] fused Wav2Vec 2.0 acoustic features with BERT transcript embeddings and ViT visual features via a BiLSTM temporal module, confirming that semantic content of speech is more discriminative than acoustic prosody alone. Collectively, these submissions converge on a modality hierarchy—text > audio > visual—that motivates our text-guided late fusion strategy.

BAH Dataset and A/H Recognition. González et al. [7] introduced the BAH dataset and established video-level multimodal baselines. Their best multimodal fusion result—LFAN co-attention [29] over all three modalities—achieves 0.59 Macro F1 at video level; zero-shot inference with a multimodal LLM [16, 30] and the full transcript reaches 0.63. Annotator cue analysis reveals that facial-language inconsistency dominates (42.6% of annotated conflict segments), followed by language-body (26.6%), providing direct empirical motivation for our explicit conflict features.

Video Representation Learning. VideoMAE [26] extends masked autoencoders to video by masking a high proportion of spatiotemporal tube patches and reconstructing pixel values, producing representations that transfer well to action recognition. We adopt VideoMAE-Base (86M parameters) pre-trained on Kinetics-400, sampling 16 frames per clip. VideoFocalNet [27] is an alternative video backbone with strong results on the BAH video-level benchmark (Macro F1 0.566) using facial crops; however, it provides visual features only and does not integrate speech or transcript.

Temporal modelling is particularly relevant for A/H recognition: hesitation cues accumulate over time [7]. Prior work employs Temporal Convolutional Networks (TCN) [3] and BiLSTM-based sequential models [8] for temporal affective modelling. In our architecture, multi-window inference—averaging predictions over five randomly sampled 16-frame windows—provides implicit temporal coverage without an explicit temporal decoder, a deliberate efficiency trade-off given the 778-sample training set.

Self-Supervised Speech Representations. HuBERT [10] learns speech representations via offline k-means cluster assignment as pseudo-labels, achieving strong performance on speech tasks without supervision. We use HuBERT-Base fine-tuned on LibriSpeech 960h (94M parameters) to encode raw 16 kHz mono audio, capturing prosodic cues—pauses, pitch variation, stuttering—that annotators identify as primary A/H indicators in the BAH codebook [7]. Wav2Vec 2.0 [1] is an alternative initially explored but replaced due to HuBERT’s superior sensitivity to expressive clinical speech.

Emotion-Aware Language Models. GoEmotions [5] is a large-scale human-annotated emotion dataset covering 27 fine-grained emotion categories including confusion, doubt, and uncertainty. SamLowe [23] fine-tuned RoBERTa-Base [15] on GoEmotions, producing a model with heightened sensitivity to hedging and hesitation language. We adopt this model as our text encoder, encoding the full video transcript rather than only the text aligned with the sampled visual window, reflecting the video-level nature of A/H: verbal hesitation indicators may occur at any point in the interview [7].

Multimodal Fusion and Conflict Modelling. Multimodal fusion strategies are broadly categorised as early (feature-level), late (decision-level), and hybrid [4]. Our approach is hybrid: a conflict-augmented early fusion stage is followed by a late blend with a unimodal text branch. Element-wise absolute differences as conflict features are motivated by disagreement-aware fusion in multimodal sentiment analysis [20] and cross-modal mismatch modelling in deception detection [19]. Compound emotion recognition—where a mixture of basic emotions is expressed simultaneously—shares the cross-modal conflict structure of A/H; C-EXPR-DB [11] demonstrates that modality representations must capture contradictions rather than consensus, directly supporting our conflict feature design.

Attention Pooling. Reducing variable-length encoder outputs to fixed-size representations is standard in multimodal pipelines. Learnable soft-attention pooling [2] assigns importance weights to each token via a learned query vector, enabling the model to upweight emotionally salient moments—vocal hesitation pauses, uncertain facial expressions—while downweighting uninformative tokens. This approach is well-established in audio-visual emotion recognition [21] and has been applied effectively to speech-based affective tasks. We employ modality-specific attention pooling for each encoder output, with padding masking for variable-length audio.

Learning from Small Affective Datasets. The BAH training set contains 778 labelled videos—a scale typical of expert-annotated clinical data. Freezing pre-trained encoder parameters and fine-tuning only task-specific heads is a well-established approach for small-data affective computing, preventing catastrophic forgetting while reducing the effective parameter count. Label smoothing [25] regularises the training signal by softening hard targets, reducing overconfidence. Threshold calibration on the validation set—selecting the operating point that maximises Macro F1 rather than defaulting to 0.5—is standard practice in binary affective challenge evaluation with class imbalance [24]. Checkpoint ensembling provides additional regularisation by averaging predictions from models trained under different regularisation settings.

3. Method

3.1. Problem Formulation

Given a video \mathcal{V} with aligned audio \mathcal{A} and a video-level speech transcript \mathcal{T} , the goal is to predict a binary label $y \in \{0, 1\}$ indicating whether Ambivalence/Hesitancy is present.

Following the challenge protocol [7], the primary metric is **Macro F1** (AVGF1): the unweighted average of F1 for the positive class (A/H present, denoted F1-AH) and F1 for the negative class (A/H absent, denoted F1-NoAH).

3.2. Multimodal Encoders

We use three modality-specific pre-trained encoders. Table 1 summarises our choices.

Table 1. Encoder backbones. All three output 768-dimensional embeddings and were selected for strong pre-trained representations while keeping the model footprint moderate.

Modality	Backbone	Params	Dim
Video	VideoMAE-Base [26]	86M	768
Audio	HuBERT-Base-LS960 [10]	94M	768
Text	RoBERTa-GoEmotions [5, 23]	125M	768

Video. We sample $T=16$ contiguous frames from each video. During training, the starting position is chosen randomly (temporal augmentation). At inference, we sample five independent windows and average their predictions (Section 3.7). All frames use the cropped-aligned faces provided by the BAH dataset and are normalised with ImageNet statistics at 224×224 resolution. VideoMAE [9] processes each sequence as pixel-value patches and outputs a token sequence of shape $(B, L_v, 768)$.

Audio. Raw 16 kHz mono audio is passed directly to HuBERT, producing a frame-level sequence $(B, L_a, 768)$. Variable-length audio is zero-padded within each batch; the

padding mask is carried forward to the attention pooling step so that padded positions do not influence the representation.

Text. The BAH dataset provides automatically generated transcripts produced using Whisper ASR [22]. The *full* video-level transcript is tokenised and encoded by RoBERTa-GoEmotions, yielding $(B, L_t, 768)$. We deliberately use the complete transcript rather than only the few seconds that correspond to the sampled video window, because A/H is a *video-level* property and hesitation cues can appear anywhere in the interview. The 27 fine-grained emotion categories of GoEmotions (e.g. confusion, nervousness, doubt) match the hedging and uncertainty vocabulary that characterises A/H, making this encoder more suitable than BERT trained only on generic text.

3.3. Attention Pooling

Each encoder produces a variable-length sequence (B, L, D) that we reduce to a single vector (B, D) via learned soft-attention pooling:

$$\alpha_i = \frac{\exp(\mathbf{w}^\top \mathbf{x}_i)}{\sum_j \exp(\mathbf{w}^\top \mathbf{x}_j)}, \quad \mathbf{e} = \sum_i \alpha_i \mathbf{x}_i, \quad (1)$$

where $\mathbf{w} \in \mathbb{R}^D$ is a learnable query vector and padding positions are masked to $-\infty$ before the softmax. A modality-specific linear projection maps each encoder’s output to the shared dimension $D=768$ before pooling. Attention pooling lets the model place more weight on the most discriminative time steps—a hesitation marker or an emotionally loaded word—rather than averaging all tokens equally.

3.4. Conflict-Aware Fusion

The central idea behind our fusion is simple: A/H is, by definition, a state of internal conflict. The person simultaneously holds opposing attitudes. We hypothesise that this internal tension leaks into observable *cross-modal disagreement*. For example, if the transcript sounds positive but the face shows stress, that mismatch *is* the signal.

To capture this, we compute pairwise absolute differences between all modality embeddings:

$$\mathbf{c}_{va} = |\mathbf{v} - \mathbf{a}|, \quad (2)$$

$$\mathbf{c}_{vt} = |\mathbf{v} - \mathbf{t}|, \quad (3)$$

$$\mathbf{c}_{at} = |\mathbf{a} - \mathbf{t}|, \quad (4)$$

where $\mathbf{v}, \mathbf{a}, \mathbf{t} \in \mathbb{R}^D$ are the pooled video, audio, and text embeddings. The absolute difference is large along dimensions where two modalities diverge, and the downstream classifier learns which of these disagreements matter for A/H prediction. This choice is motivated by the BAH annotator analysis [7], which shows that face–language inconsistency accounts for 42.6% of annotator cues. Absolute

difference has also proven effective for cross-modal inconsistency in sentiment analysis [20].

Note that the modality-specific projections are learned end-to-end and are not pre-aligned through contrastive objectives (e.g. CLIP-style pre-training). The alignment emerges entirely from the classification signal.

The full fusion representation concatenates modality and conflict features:

$$\mathbf{f} = [\mathbf{v}; \mathbf{a}; \mathbf{t}; \mathbf{c}_{va}; \mathbf{c}_{vt}; \mathbf{c}_{at}] \in \mathbb{R}^{6D}. \quad (5)$$

A two-layer feed-forward network (LayerNorm, Linear→GELU→Dropout, hidden width $2 \times 6D$) processes this vector, followed by a classification MLP head: LayerNorm → Linear($6D, 512$) → GELU → Dropout(0.3) → Linear($512, 1$), producing the full-fusion logit $\ell_{\text{full}} \in \mathbb{R}$.

3.5. Text-Guided Late Fusion

Text carries the strongest discriminative signal for A/H—a finding reported by Savchenko [24] and confirmed by our own modality ablation (Table 5). Rather than ignoring this and hoping the multimodal path figures it out, we make it explicit with a parallel *text-only auxiliary head* [14]:

$$\ell_{\text{text}} = \text{MLP}_{\text{text}}(\mathbf{t}), \quad (6)$$

identical in architecture to the full-fusion head but operating only on $\mathbf{t} \in \mathbb{R}^D$.

Why does this help? On a small dataset like BAH (778 training videos), the multimodal path can overfit to noisy visual or acoustic patterns. The text-only head acts as a regulariser: it forces the shared text encoder to produce embeddings that are independently discriminative, not just useful when combined with other modalities.

Training. Both heads are trained jointly with balanced loss weights:

$$\tilde{y} = y(1 - \varepsilon) + 0.5\varepsilon, \quad (7)$$

$$\mathcal{L} = (1 - w) \text{BCE}(\ell_{\text{full}}, \tilde{y}) + w \text{BCE}(\ell_{\text{text}}, \tilde{y}), \quad (8)$$

where $w=0.5$ and ε is a label-smoothing parameter ($\varepsilon=0.1$ or 0 depending on the checkpoint configuration; see Section 4.2).

Inference. At test time the two branches are blended:

$$p = \alpha \cdot \sigma(\ell_{\text{text}}) + (1 - \alpha) \cdot \sigma(\ell_{\text{full}}), \quad (9)$$

where σ is the sigmoid function and $\alpha=0.6$, tuned on the validation set. The weight $\alpha > 0.5$ reflects the text branch’s stronger predictive power while still incorporating multimodal evidence.

3.6. Architecture Overview

Figure 1 gives a high-level view of the full pipeline.

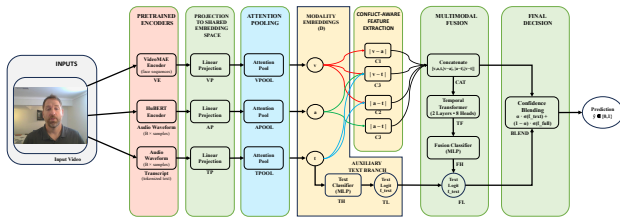


Figure 1. **ConflictAwareAH architecture.** Video frames, audio waveform, and transcript pass through pre-trained encoders and attention pooling to produce embeddings \mathbf{v} , \mathbf{a} , \mathbf{t} . Three pairwise conflict vectors are concatenated with the modality embeddings and fed to a two-layer FFN, producing the full-fusion logit l_{full} . A parallel text-only head produces l_{text} . At inference the two are blended via Eq. 9.

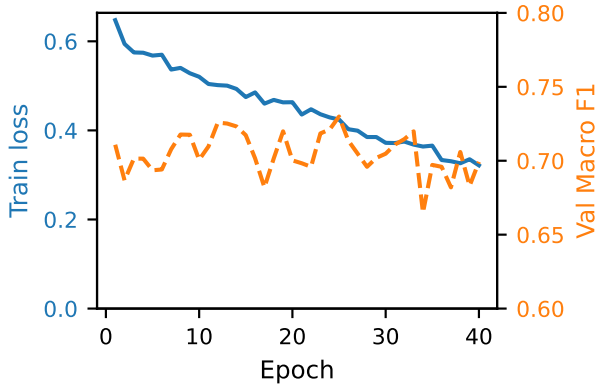


Figure 2. Train loss and validation Macro F1 over epochs (Run A).

3.7. Training Protocol

Optimiser. AdamW ($\beta_1=0.9$, $\beta_2=0.999$, weight decay 10^{-2}) with learning rate 3×10^{-5} and cosine annealing to 3×10^{-7} . Mixed precision (fp16) is used throughout.

Batch size. We use mini-batches of 4, accumulated over 4 gradient steps for an effective batch size of 16.

Encoder freezing. Given only 778 training samples, we freeze all encoder weights by default. The top-2 Transformer layers of each encoder are optionally unfrozen at a $10 \times$ lower learning rate (3×10^{-6}) for gentle adaptation.

Class weighting. We re-weight BCEWithLogitsLoss by the inverse positive-class frequency (pos_weight ≈ 0.96).

Early stopping. Training stops when Macro F1 on the validation set does not improve for 15 consecutive epochs (max 60 epochs). Figure 2 shows typical train loss and validation Macro F1 curves; train/val divergence after epoch 17–19 indicates overfitting.

Threshold tuning. After each epoch we sweep thresholds

in $[0.25, 0.75]$ at 0.01 resolution on the blended validation probabilities. The best threshold from the checkpoint with peak Macro F1 is used at test time.

Multi-window inference. At test time, instead of a single 16-frame window, we can sample N random contiguous windows per video and average the resulting probabilities. This gives broader visual coverage over the whole interview, better matching the temporal scope of the full transcript. We use $N=5$ in our submitted results.

4. Experiments

4.1. Dataset

All experiments use the BAH dataset provided for the ABAW10 challenge [7, 13]. It contains 1,427 videos (10.6 hours, $\sim 27s$ per video on average) from 300 Canadian participants. Each video has video-level and frame-level A/H annotations, a speech-to-text transcript, and participant metadata. Splits are made at the participant level so that no person appears in both training and evaluation. Table 2 shows the statistics.

Table 2. BAH dataset split statistics for the ABAW10 A/H challenge.

Split	Videos	A/H (+)	No A/H (-)
Train	778	385 (49%)	393 (51%)
Val	124	75 (60%)	49 (40%)
Test	525	318 (61%)	207 (39%)
Test (unlabeled)	161	—	—

4.2. Implementation Details

All experiments run on a single NVIDIA RTX 4090 GPU (24GB). Pre-trained weights come from the HuggingFace Model Hub. Training one epoch takes roughly 50 seconds; a typical run converges in 20–25 minutes.

For our final submission we use an *ensemble of two checkpoints*, each trained with the same architecture but different regularisation settings:

- **Checkpoint A:** top-2 encoder layers unfrozen, no label smoothing ($\epsilon=0$).
- **Checkpoint B:** all encoder layers fully frozen, label smoothing with $\epsilon=0.1$.

The two models produce complementary predictions: Checkpoint A benefits from task-specific encoder adaptation while Checkpoint B is more stable and less prone to overfitting. At test time, we average the sigmoid probabilities from both checkpoints (each using 5-window inference) and then apply the best validation threshold. The code is implemented in PyTorch [18] with HuggingFace Transformers [28].

4.3. Main Results

Table 3 compares ConflictAwareAH against published baselines.

Table 3. Comparison on the ABAW10 A/H test split (525 videos). BAH baselines are from González et al. [7].

Method	Macro F1
BAH: Zero-shot M-LLM (vision only) [7]	0.283
BAH: Video-FocalNet base [7]	0.566
BAH: LFAN (V+A+T, co-attention) [7]	0.593
BAH: Zero-shot M-LLM + transcript [7]	0.634
Ours — single model (1 or 5 windows)	0.690–0.692
Ours — ensemble (2 ckpts × 5 win.)	0.694

A single ConflictAwareAH model already outperforms the strongest BAH baseline (M-LLM + transcript, 0.634) by +5.6 points. The two-checkpoint ensemble pushes this to 0.694. Importantly, training a single model takes under 25 minutes on one RTX 4090 GPU—no multi-node training, no large-scale fine-tuning.

On the private **test_unlabeled** split (161 videos, labels withheld), our submitted ensemble obtained an official Macro F1 of **0.715** in the ABAW10 challenge evaluation. The improvement from 0.694 (labelled test) to 0.715 (private test) suggests the model generalises robustly to unseen participants.

4.4. Ablation Studies

We now examine each component of our design through systematic ablations. Unless stated otherwise, experiments use the full model with $\alpha=0.6$ (text blend), top-2 layer un-freezing, no label smoothing, and single-window inference on the test split.

How much does the text blend help? Table 4 answers this question. Setting $\alpha=0.0$ (full-fusion only, no text branch at inference) gives 0.649 Macro F1. Blending with $\alpha=0.6$ raises this to 0.690: a **+4.1 point gain** from a single hyperparameter. In fact, using the text head alone ($\alpha=1.0$) achieves 0.700, the best single-branch score. The text-guided blend is clearly the primary driver of our performance.

Do conflict features help? Removing the three conflict vectors and feeding only [v; a; t] to the fusion network yields 0.681. Our full model (0.690) outperforms this by **+0.9 points**, indicating that the explicit conflict features contribute to the model’s discriminative ability. While the gain is modest, it is consistent with the hypothesis that cross-modal disagreement carries a meaningful signal for A/H.

Full transcript vs. window-aligned text. Restricting the text to only the seconds matching the video window gives 0.698, comparable to using the full transcript (0.690). We use the full transcript by default since A/H is a video-level label and hesitation markers can occur at any point in the interview.

Table 4. Component ablation on the test split.

Configuration	Macro F1
No conflict features (v+a+t only)	0.681
Window-aligned transcript only	0.698
Text blend $\alpha = 0.0$ (full-fusion only)	0.649
Text blend $\alpha = 0.5$	0.689
Text blend $\alpha = 0.6$ (ours)	0.690
Text blend $\alpha = 1.0$ (text-only at inference)	0.700

Which modalities matter most? Table 5 breaks this down on the validation split. Text alone reaches 0.737 Macro F1—far above video (0.534) or audio (0.523). Combining all three modalities (0.746) yields a modest gain over text only (+0.9 points). Adding video or audio to text does not hurt, but the improvement is small, reflecting the strong dominance of the linguistic channel for this task. However, multimodal cues do improve robustness when linguistic signals are ambiguous—for instance during pauses, filled hesitations, or when the transcript is noisy.

Table 5. Modality ablation (validation split, 124 videos).

Modality	Macro F1	F1-AH	F1-NoAH
Video only	0.534	0.560	0.508
Audio only	0.523	0.645	0.400
Text only	0.737	0.804	0.670
Video + Audio	0.527	0.573	0.481
Video + Text	0.734	0.783	0.685
Audio + Text	0.736	0.789	0.683
All three (ours)	0.746	0.777	0.716

Inference windows and ensembling. Table 6 shows how multi-window inference and checkpoint ensembling affect the test score. Going from 1 window to 5 windows has marginal effect on its own, but the two-checkpoint ensemble consistently provides the best result (0.694), likely because the two checkpoints are trained with different regularisation and therefore make different errors.

4.5. Analysis and Discussion

Text dominates—but is biased. The ablation results tell a consistent story: text is the most informative individ-

Table 6. Inference settings on the test split.

Setting	Macro F1
Inference: 1 window	0.692
Inference: 3 windows	0.690
Inference: 5 windows (ours)	0.690
Single checkpoint (5 windows)	0.690
Ensemble of 2 checkpoints (5 win.)	0.694

ual modality for A/H recognition. Using only the text branch at inference ($\alpha=1.0$) reaches 0.700 Macro F1, higher than full-fusion only ($\alpha=0.0$, 0.649). However, a closer look at Table 5 reveals a systematic weakness: text-only achieves high F1-AH (0.804) but substantially lower F1-NoAH (0.670), yielding a class-performance gap of 0.134. The model over-detects A/H because hedging and uncertainty language is common in clinical interviews even when no genuine ambivalence is present. In contrast, our full conflict-aware model narrows this gap to 0.061 (F1-AH 0.777, F1-NoAH 0.716), improving F1-NoAH by **+4.6 points** while sacrificing only 2.7 points on F1-AH. This rebalancing is clinically important: in deployment, false-positive A/H flags waste clinician time, so a model that reliably confirms the *absence* of ambivalence is at least as valuable as one that detects its presence.

Conflict features as a bidirectional signal. The class-bias correction above is driven by the conflict features. When the modality embeddings $agree=|v - t|$ is small—the conflict vector provides an explicit consistency cue that anchors the negative class. A text-only approach has no mechanism to verify whether verbal content matches facial and prosodic behaviour; it can detect hesitant *language* but cannot confirm behavioural *consistency*. Conversely, when the transcript expresses certainty (e.g. “I’m totally fine with it”) but the face shows micro-expressions of stress, the conflict vector is large along the relevant dimensions and the classifier correctly flags A/H. Thus, the conflict features act as a bidirectional signal: disagreement flags A/H, agreement confirms No A/H. On the aggregate metric, this appears as a modest +0.9 Macro F1 (Table 4); the per-class breakdown reveals that the real contribution is a substantially better-calibrated model.

Text-guided late fusion complements conflict features. Text-guided late fusion adds +4.1 Macro F1 by allowing the system to rely on the text head when its linguistic signal is confident, while still having access to multimodal and conflict-based evidence for harder cases. The two mechanisms address different failure modes: conflict features correct class bias, while text-guided blending boosts overall discriminability.

Robustness beyond text. Relying exclusively on text introduces additional risks in clinical deployment. Automatic transcripts are generated by Whisper ASR [22], which can produce errors on accented, mumbled, or overlapping clinical speech. Silent or minimally verbal patients—especially those exhibiting non-verbal A/H cues—would yield uninformative transcripts. Moreover, clinicians primarily assess A/H through visual and prosodic cues (the BAH annotator analysis attributes 42.6% of cues to facial–language inconsistency [7]). A multimodal conflict-aware system aligns more closely with clinical practice than a text-only approach.

Overfitting is the main challenge. With 778 training samples and potentially 60M trainable parameters (when encoder layers are unfrozen), the train–validation loss curves diverge after epoch 17–19. Freezing all encoder layers and applying label smoothing produces comparable peak performance with faster convergence and smaller generalisation gaps, making it the safer choice at this data scale.

Limitations. First, threshold tuning on the validation set may not transfer perfectly if the test distribution shifts significantly; we report both splits for transparency. Second, the 16-frame window captures only a small portion of each video; multi-window inference alleviates this but does not fully solve temporal modelling. Third, the modality embeddings are not pre-aligned through contrastive objectives; the absolute-difference conflict features therefore capture geometric rather than semantic distance, and richer conflict representations (e.g. cross-attention between modalities or projected differences in a shared space) are a promising direction for future work.

5. Conclusion

We presented ConflictAwareAH, a multimodal framework for recognising Ambivalence and Hesitancy in clinical interview videos. The key insight is that while text is the most discriminative individual modality for A/H, it is also systematically biased: text-only models over-detect A/H while struggling to confirm its absence.

Our main contribution, *conflict-aware fusion*, addresses this through explicit pairwise cross-modal difference features. These features serve as bidirectional cues—large differences flag A/H while small differences anchor the negative class—improving F1-NoAH by +4.6 points and halving the class-performance gap compared to text alone. A complementary *text-guided late fusion* strategy adds +4.1 Macro F1 by blending a text-only auxiliary head with the full multimodal output. Our best result (0.694 Macro F1 on the labelled test split, 0.715 on the ABAW10 private leaderboard) comes from ensembling two checkpoints trained with com-

plementary regularisation and averaging predictions over multiple inference windows.

The system outperforms all published BAH multimodal baselines (best: 0.593) and the zero-shot M-LLM with transcript (0.634), and it trains in under 25 minutes on a single GPU.

Three directions for future investigation stand out: (1) alignment-aware conflict representations through contrastive pre-training or cross-attention, which may amplify the bidirectional signal; (2) temporal modelling across multiple video segments, where a Transformer attends over N independent clip representations instead of averaging them; and (3) richer regularisation strategies (e.g. mixup, stochastic depth, or parameter-efficient fine-tuning) to push performance further on datasets of this scale.

References

- [1] Alexei Baevski, Henry Zhou, Abdelrahman Mohamed, and Michael Auli. wav2vec 2.0: A framework for self-supervised learning of speech representations. In *Advances in Neural Information Processing Systems (NeurIPS)*, 2020. 3
- [2] Dzmitry Bahdanau, Kyunghyun Cho, and Yoshua Bengio. Neural machine translation by jointly learning to align and translate. In *International Conference on Learning Representations (ICLR)*, 2015. 3
- [3] Shaojie Bai, J. Zico Kolter, and Vladlen Koltun. An empirical evaluation of generic convolutional and recurrent networks for sequence modeling. *arXiv preprint arXiv:1803.01271*, 2018. 2
- [4] Tadas Baltrušaitis, Chaitanya Ahuja, and Louis-Philippe Morency. Multimodal machine learning: A survey and taxonomy. *IEEE Transactions on Pattern Analysis and Machine Intelligence*, 41(2):423–443, 2019. 3
- [5] Dorottya Demszky, Dana Movshovitz-Attias, Jeongwoo Ko, Alan Cowen, Gaurav Nemade, and Sujith Ravi. GoEmotions: A dataset of fine-grained emotions. In *Proceedings of the Annual Meeting of the Association for Computational Linguistics (ACL)*, 2020. 3
- [6] Daniel Freeman, Bao S. Loe, Andrew Chadwick, Cristian Vaccari, Felicity Waite, Laina Rosebrock, et al. COVID-19 vaccine hesitancy in the UK: the oxford coronavirus explanations, attitudes, and narratives survey (OCEANS) II. *Psychological Medicine*, 52(14):3127–3141, 2021. 2
- [7] Manuela González-González, Soufiane Belharbi, Muhammad Osama Zeeshan, Masoumeh Sharafi, Muhammad Haseeb Aslam, Marco Pedersoli, Alessandro Lameiras Koerich, Simon L. Bacon, and Eric Granger. BAH dataset for ambivalence/hesitancy recognition in videos for digital behavioural change. In *International Conference on Learning Representations (ICLR)*, 2026. 2, 3, 4, 5, 6, 7
- [8] Erik Hallmen et al. Semantic matters: Multimodal features for affective analysis at the ABAW-8 competition. In *Proceedings of the IEEE/CVF Conference on Computer Vision and Pattern Recognition Workshops (CVPRW)*, 2025. ABAW Workshop at CVPR 2025. 2
- [9] Kaiming He, Xinlei Chen, Saining Xie, Yanghao Li, Piotr Dollár, and Ross Girshick. Masked autoencoders are scalable vision learners. In *Proceedings of the IEEE/CVF Conference on Computer Vision and Pattern Recognition (CVPR)*, pages 16000–16009, 2022. 3
- [10] Wei-Ning Hsu, Benjamin Bolte, Yao-Hung Hubert Tsai, Kushal Lakhotia, Ruslan Salakhutdinov, and Abdelrahman Mohamed. HuBERT: Self-supervised speech representation learning by masked prediction of hidden units. *IEEE/ACM Transactions on Audio, Speech, and Language Processing*, 29:3451–3460, 2021. 3
- [11] Dimitrios Kollias. Multi-label compound expression recognition: C-EXPR database & network. In *Proceedings of the IEEE/CVF Conference on Computer Vision and Pattern Recognition (CVPR)*, 2023. 3
- [12] Dimitrios Kollias, S. Cheng, and S. Zafeiriou. ABAW: Learning from synthetic data & compound expression recognition. In *Proceedings of the IEEE/CVF Conference on Computer Vision and Pattern Recognition Workshops (CVPRW)*, 2024. 2
- [13] Dimitrios Kollias et al. ABAW: Affective behavior analysis in-the-wild — 10th challenge. In *Proceedings of the IEEE/CVF Conference on Computer Vision and Pattern Recognition Workshops (CVPRW)*, 2026. Challenge description paper. 2, 5
- [14] Kevin Liang, Jing Zhang, et al. Improved multimodal fusion for small datasets with auxiliary supervision. In *Medical Image Computing and Computer-Assisted Intervention (MICCAI)*, 2024. 4
- [15] Yinhan Liu, Myle Ott, Naman Goyal, Jingfei Du, Mandar Joshi, Danqi Chen, Omer Levy, Mike Lewis, Luke Zettlemoyer, and Veselin Stoyanov. RoBERTa: A robustly optimized BERT pretraining approach. 2019. 3
- [16] Yiqun Luo et al. Multimodal large language models for affective computing: A comprehensive survey. *arXiv preprint arXiv:2501.09688*, 2025. 2
- [17] William R. Miller and Stephen Rollnick. *Motivational Interviewing: Helping People Change*. Guilford Press, 3rd edition, 2012. 2
- [18] Adam Paszke, Sam Gross, Francisco Massa, Adam Lerer, James Bradbury, Gregory Chanan, Trevor Killeen, Zeming Lin, Natalia Gimelshein, Luca Antiga, et al. PyTorch: An imperative style, high-performance deep learning library. In *Advances in Neural Information Processing Systems (NeurIPS)*, 2019. 5
- [19] Verónica Pérez-Rosas, Mohamed Abouelenien, Rada Mihalcea, Yao Xiao, C J Linton, and Mihai Burzo. Verbal and nonverbal clues for real-life deception detection. In *Proceedings of the 2015 Conference on Empirical Methods in Natural Language Processing (EMNLP)*, pages 2336–2346, 2015. 3
- [20] Soujanya Poria, Erik Cambria, Devamanyu Hazarika, Navonil Majumder, Amir Zadeh, and Louis-Philippe Morency. Context-dependent sentiment analysis in user-generated videos. In *Proceedings of the Annual Meeting of the Association for Computational Linguistics (ACL)*, 2017. 3, 4

- [21] R. Gnana Praveen, Eric Granger, and Marco Pedersoli. A joint cross-attention model for audio-visual fusion in dimensional emotion recognition. *IEEE Transactions on Biometrics, Behavior, and Identity Science (TBIOM)*, 5(3):446–459, 2023. 3
- [22] Alec Radford, Jong Wook Kim, Tao Xu, Greg Brockman, Christine McLeavey, and Ilya Sutskever. Robust speech recognition via large-scale weak supervision. In *International Conference on Machine Learning (ICML)*, 2023. 4, 7
- [23] SamLowe. roberta-base-go.emotions. https://huggingface.co/SamLowe/roberta-base-go_emotions, 2022. 3
- [24] Andrey V. Savchenko. Facial expression recognition and ambivalence/hesitancy recognition at the 8th ABAW competition. In *Proceedings of the IEEE/CVF Conference on Computer Vision and Pattern Recognition Workshops (CVPRW)*, 2024. 2, 3, 4
- [25] Christian Szegedy, Vincent Vanhoucke, Sergey Ioffe, Jon Shlens, and Zbigniew Wojna. Rethinking the inception architecture for computer vision. In *Proceedings of the IEEE/CVF Conference on Computer Vision and Pattern Recognition (CVPR)*, pages 2818–2826, 2016. 3
- [26] Zhan Tong, Yibing Song, Jue Wang, and Limin Wang. VideoMAE: Masked autoencoders are data-efficient learners for self-supervised video pre-training. In *Advances in Neural Information Processing Systems (NeurIPS)*, 2022. 2, 3
- [27] Syed Talal Wasim, Muhammad Uzair Khattak, Muzammal Naseer, Salman Khan, Mubarak Shah, and Fahad Shahbaz Khan. Video-FocalNets: Spatio-temporal focal modulation for video action recognition. In *Proceedings of the IEEE/CVF International Conference on Computer Vision (ICCV)*, 2023. 2
- [28] Thomas Wolf, Lysandre Debut, Victor Sanh, Julien Chaumond, Clement Delangue, Anthony Moi, et al. Transformers: State-of-the-art natural language processing. In *Proceedings of the 2020 Conference on Empirical Methods in Natural Language Processing: System Demonstrations (EMNLP)*, pages 38–45, 2020. 5
- [29] Haiyang Zhang, Yanyan Wang, Ziqiang Zhang, Bing Liu, et al. LFAN: Lightweight fusion attention network for multi-modal sentiment analysis. In *IEEE International Conference on Acoustics, Speech and Signal Processing (ICASSP)*, 2023. 2
- [30] Zheng Zhang, Ziwei Liu, Fangshuo Hong, et al. GPT-4V with emotion: A zero-shot benchmark for generalized emotion recognition. *arXiv preprint arXiv:2312.04293*, 2024. 2